Chance and pleiotropy dominate genetic diversity in complex bacterial environments

Lianet Noda-Garcia[1], Dan Davidi[2], Elisa Korenblum[2], Assaf Elazar[1], Ekaterina Putintseva[3], Asaph Aharoni[2] & Dan S. Tawfik[1,*]

[1]Department of Biomolecular Sciences, Weizmann Institute of Science, Rehovot 76100, Israel.

[2]Department of Plant and Environmental Sciences, Weizmann Institute of Science, Rehovot 76100, Israel.

[3]Institutes of Science and Technology, Klosterneuburg, Austria.

* Corresponding author; e-mail: dan.tawfik@weizmann.ac.il.

Abstract

How does environmental complexity affect the evolution of single genes? Here, we measured the effects of a set of mutants of *Bacillus subtilis* glutamate dehydrogenase across 19 different environments – from homogenous single cell populations in liquid media to heterogeneous biofilms, plant roots and soil communities. The effects of individual gene mutations on organismal fitness were highly reproducible in liquid cultures. Strikingly, however, 84% of the tested alleles showed opposing fitness effects under different carbon and nitrogen sources (antagonistic pleiotropy). In biofilms and soil samples, different alleles dominated in parallel replica experiments. Accordingly, we found that in these heterogeneous bacterial communities the fate of mutations was dictated by a combination of selection and drift. The latter was driven by programmed prophage excisions that occurred along biofilm development. Overall, per individual condition, by the combined action of selection, pleiotropy and chance, a wide range of glutamate dehydrogenase mutations persisted and sometimes fixated. However, across longer periods and multiple environments nearly all this diversity would be lost – indeed, considering all environments and conditions we have tested, wild-type is the fittest allele.

38 The function of most genes may be essential in some conditions, but only
39 marginally contributing, or even redundant, in other conditions [1–4]. The effects of
40 mutations on organismal fitness are therefore environment-dependent, giving
41 rise to complex, pleiotropic genotype-by-environment interactions [5,6]. Moreover,
42 bacterial populations often do not comprise single cells, but rather have a
43 structure as in biofilms. Under this complexity: changing environments and
44 heterogeneous bacterial communities, the fate of mutations could also be
45 dictated by population bottlenecks (drift) or rapid takeover of beneficial
46 mutations in other genes (selective sweeps) [7–9].Consequently, the frequency of a
47 given gene allele may change dramatically (from perishing to fixation) with no
48 relation to its molecular function [10,11].

49 We aimed at an experimental setup would examine how complex
50 bacterial growth states and environments might shape protein evolution.
51 Previous systematic mappings were based on a direct linkage between protein
52 stability and function and organismal survival, thus enabling measurements of
53 effects of mutations at the protein level [5,12–15]. However, how mutations in a
54 single gene-protein affect organismal fitness under varying environments and
55 conditions is largely unexplored [16]. We thus chose as our model *Bacillus subtilis*
56 NCIB 3610, a non-domesticated strain capable of growing in diverse aquatic and
57 terrestrial environments [17]. We explored the effects of mutations in different
58 conditions: in dispersed cells in liquid, but also in biofilms where phenotypic and
59 genetic variability prevails [18]. We also mapped the effects of mutations during
60 spore formation and germination [19] and in more complex and close to natural
61 environments including soil, rhizosphere and plant roots.

62 A catabolic glutamate dehydrogenase (GDH) was our model protein. This
63 enzyme is essential when amino acids such as proline serve as sole carbon-
64 nitrogen sources [20]. However, in the presence of ammonia and glycolytic sugars,
65 GDH activity is redundant as glutamate must be synthesized rather than
66 catabolized. GDHs therefore respond to changes in carbon-nitrogen sources, and
67 as regulators of glutamate homeostasis, are also associated with biofilm
68 development [21,22]. *B. subtilis* has two catabolic GDHs, RocG and GudB. The latter
69 is constitutively expressed, and is regulated via association of its hexameric form
70 [23]. GudB has also regulatory roles [24,25] via interactions with the transcriptional
71 activator of glutamate synthase [25] and with an essential transcription
72 termination factor, NusA, that also modulates the stringent response [26–28]. We
73 explored mutations in the oligomeric interface of GudB, aiming at multilateral
74 effects on GudB's enzymatic and regulatory functions.
75 Altogether, these choices of organism and enzyme allowed us to readily
76 examine and quantify the fate of GudB alleles in a range of different growth
77 conditions and environments, also mimicking natural habitats where strong
78 evolutionary forces act [11].
79
80 **Experimental setup and data processing**
81 We anticipated that the effects of the explored mutations would be complex and
82 condition-dependent. We thus opted for high rather than broad coverage and
83 mapped 10 positions within a single ~150 base pairs segment that resides at
84 GudB's oligomeric interface while choosing highly conserved (D58) as well as
85 highly diverged positions (M48, or S61; **Table S1**). Positions were diversified
86 using NNS (whereby N represents any of the 4 bases, and S, G or C). The resulting

87 GudB library contained in total 320 single mutant alleles (including wild-type),
88 whose genomes differ, in principle, by a single mutation: 200 different amino
89 acid alleles and 10 stop-codons. The library therefore included synonymous
90 alleles whereby the same amino acid was encoded by 2 or 3 different codons.
91 This allele library was incorporated into the chromosome of *B. subtilis* NCIB
92 3610 under *gudB*'s original promoter and terminator.

93 This starting population (the initial mix, hereafter) was used to inoculate
94 cultures grown in an array of different conditions. We tested 7 different growth
95 states where the population complexity varies from single cells to community:
96 liquid, pellicles (air-liquid biofilms), spores, germinated spores, biofilms grown
97 on agar including on carbon-nitrogen gradients, and soil colonization. Up to 5
98 different carbon-nitrogen sources were used that, at least as far as the
99 phenotypes of the GudB knockout indicate, inflict different levels of selection on
100 GudB: Glutamate *plus* ammonia (GA), where ΔGudB has no growth effect;
101 glutamate *plus* glycerol (GG), arginine (A), and arginine *plus* proline (PA), where
102 ΔGudB exhibits a slight growth defect, and proline (P), where ΔGudB exhibits the
103 strongest growth defect (**Fig. S1**). Thus, in total, we tested 19 conditions. At each
104 condition, three to five biological replicas were performed by inoculating from
105 the same initial mix. The cultures were grown in parallel, and individually
106 analyzed. Illumina sequencing was applied to determine the frequency of each of
107 the *gudB* alleles in the initial mix and after growth. Following filtering (see
108 Methods), we obtained data for 244 up to 269 individual alleles per experiment
109 (**Data S1** & **Fig. S2)**.

110 The ratio between an allele's frequency at the end of growth and in the
111 initial mix was derived, and this ratio is referred to as the frequency coefficient

112 (FC; **Data S2**). Given the experimental error in determining FC values, values
113 between 0.8 and 1.2 were classified as 'neutral', FC ≤0.8 assigned a mutation as
114 'deleterious', and FC >1.2 as 'beneficial'. Mutations with FC ≤0.1 were classified
115 as 'highly deleterious', and similarly, FC ≥10 as 'highly beneficial' (see Methods).
116 Note that the number of generations in liquid growth (~50 generations) and
117 spores (a dormant non-replicative form of *B. subtilis*), for example, differs
118 fundamentally. Moreover, in pellicles and biofilms, the number of generations
119 cannot be readily determined –different cell types having different growth rates
120 [29]. So, while we could not calculate selection coefficients (*s*), one should keep in
121 mind that an FC value of 0.8 in the spores is in effect equivalent to extinction
122 across 50 generations in liquid ($0.8^{50} = 10^{-5}$).
123

124 **Irreproducibility – selection *versus* drift**

125 Our first observations indicate two contrasting scenarios. In liquid cultures, for
126 example, we observed highly reproducible FC values in biological replicas (**Fig.**
127 **1a**). Given the small sample numbers (3 replicas, 5 in few cases like the
128 rhizosphere), the observed variance may underestimate the actual variance.
129 However, the repetitively low variance levels in a range of different liquid
130 conditions, and in other replica measurements in liquid [30], supports high
131 reproducibility. In biofilms, however, despite the fact that we did not bottleneck
132 any population upon inoculum, the correlation between replicas was very low
133 **(Fig. 1b**). The reproducibility between biological replicas indicates selection,
134 thus indicating that that protein and organismal fitness are tightly coupled. In
135 biofilms however, the lack of reproducibility indicates the dominance of drift, i.e.,
136 random sampling of GudB alleles.

To quantify the contribution of selection versus drift in different conditions, we used two criteria. Firstly, we compared the variability in FC values between replicas by calculating the standard deviation (SD) per allele (using the logarithm of the FC values; see Methods). The average SD value for all alleles in each experiment ($\overline{SD}$) is given for 7 general growth states (**Fig. 1c; Fig. S3a** & **Table S2**). As can be seen, in liquid, pellicles and spores, the $\overline{SD}$ values between biological replicas were low (< 0.06). In biofilms and bulk soil, however, the $\overline{SD}$ values were > 0.25 indicating low reproducibility.

Secondly, if drift dictates the fate of GudB alleles, codons of the same amino acid would exhibit very different FC values. The deviations between synonymous codons of the same amino acid alleles were calculated, averaged for all alleles in the same experiment, and then for all replica experiments per condition ($\overline{SD}$syn, in log values; **Fig. 1d; Fig. S3b** & **Table S3**). Note that the $\overline{SD}$syn criterion holds within individual replica experiments and is thus independent of the comparison of $\overline{SD}$ between biological replicas. Nonetheless, these criteria are clearly correlated (**Fig. 1c** & **d**). Overall, it appears that in liquid, pellicles and spores, the FC values report the outcome of selection acting on GudB alleles at the amino acid level as expected (in few alleles, selection also acted reproducibly at the codon level, **Fig. S4**). In contrast, in biofilms and bulk soil we consistently observed higher $\overline{SD}$ and $\overline{SD}$syn values. In some biofilm experiments, the $\overline{SD}$syn values exceeded 3 (*i.e.*, > 10^3 SD values on a liner scale). Thus, in effect, a single codon had taken over.

Given that some conditions were selection-dominated and others are subject to chance, we divided our analysis in two. Firstly, we analyzed selection

161 dominated conditions (liquid, pellicles and spores) to examine whether and how
162 the fate of GudB mutations change under different environments. Secondly,
163 conditions where drift prevailed (germination, biofilms and soil colonization)
164 were analyzed to reveal the relative contributions of selection *versus* chance and
165 the molecular mechanisms of drift.
166
167 **Pleiotropy - fitness-effects of mutations are condition-dependent**
168 While the FC values, and hence the fitness effects of mutations, were
169 reproducible under many conditions, their distribution varied widely between
170 conditions, including between carbon-nitrogen sources (**Fig. S5**). This indicates
171 pleiotropy – individual GudB alleles have different fitness effects in different
172 conditions. To quantify the level of pleiotropy, we compared the FC values of the
173 same GudB mutation across the 9 individual selection-dominated conditions.
174 Because the number of generations differs from one condition to another, we
175 focused on shift from beneficial to deleterious, and vice versa (sign, or
176 antagonistic pleiotropy) as the sign of the FC values of mutations indicates their
177 fitness sign irrespective of generation numbers. Representative dot plots
178 comparing the FC values across 3 different liquid conditions are shown (**Fig. 2a**).
179 These indicate that pleiotropy is common, even when comparing liquid cultures
180 with overlapping carbon-nitrogen sources. In particular, a significant number of
181 GudB mutations show antagonistic pleiotropy (dashed squares, **Fig. 2a**). Indeed,
182 the Pearson correlation values for the 36 possible pair-wise comparisons of 9
183 conditions were below 0.7 (**Fig. 2b**). Across all selection-dominated conditions,
184 up to 84% of alleles showed antagonistic pleiotropy in one or more of the 36 pair
185 wise comparisons, and 70% of alleles showed mild or strong antagonistic

186 pleiotropy. These pleiotropic effects are far beyond experimental noise, as
187 indicated by comparison to a control sample (**Fig. 2c**).

188 Overall, the dominance of pleiotropy meant that across all protein –
189 organismal fitness coupled conditions, 86% of the alleles were beneficial in at
190 least one condition. However, not a single mutation was beneficial across all
191 conditions. Further, if a mutation were to be considered deleterious if it was
192 purged in at least one condition, then 98% of the tested GudB mutations were
193 deleterious. To our knowledge, the degree of pleiotropy in protein mutations
194 across multiple environments has not been measured so far. The exceedingly
195 high degree of pleiotropy we found may relate to GudB's multiple roles, as an
196 enzyme and regulator, and also to the chosen mutated positions (oligomer
197 interface), but it may well be a general characteristic of proteins with key
198 physiological roles. In some samples, only two alleles were present at >1%
199 frequency, one being wild-type (**Fig. 3** & **Data S1**). The near-fixation of relatively
200 few alleles could indicate very strong selection acting on GudB. However, the
201 high $\overline{SD}$ and exceedingly high $\overline{SD}$syn values suggest fixation by chance (**Fig. 1c** &
202 **d**). What is then the nature of these few GudB 'winners', are they merely lucky?
203

204 **Combined action of selection and drift in heterogeneous environments**

205 While drift dominated in biofilms and soil colonization, curiously, wild type
206 GudB was enriched in up to 85% of these experiments suggesting that selection
207 does play a role (**Fig. 3**). To assess the action of selection, we compared the three
208 biofilm areas. There appears a systematic trend, whereby enriched alleles in the
209 edge are more likely to arise from alleles that persisted or even enriched in the
210 center (**Fig. 4a**). Similarly, although gradient biofilms were clearly dominated by

211 drift, 75% of the enriched alleles were neutral or beneficial under liquid growth
212 with proline, a condition under which GudB experiences the strongest selection
213 (**Fig. 4b**). This suggested that GudB is under selection at the early stages of
214 biofilm development. Accordingly, we found that in biofilm centers, the FC values
215 are less skewed and more reproducible (**Fig. S5**), and also, the center $\overline{SD}$syn
216 values are half than in the edge or wrinkles (**Table S3** & **Fig. S3b**). The $\overline{SD}$syn
217 values are obviously higher in the biofilms' center compared to liquid cultures,
218 but the trend suggests that at the onset of the biofilm's development, selection
219 acts on GudB (**Table S3** & **Fig. S3b**).

220 Similarly, we tested for signatures of selection in soil colonization. As in
221 biofilms, there is a statistically significant trend, whereby enriched alleles in the
222 root are more likely to arise from alleles that were enriched in the soil (**Fig. 4c**).
223 Further, 19 amino acid substitutions were enriched in at least 10 out of the 15
224 sequenced populations, suggesting reproducibility. Of these, in two amino acid
225 alleles, both synonymous codons enriched (D59A and D59V; $\overline{SD}$syn = 0.42 and
226 0.35; **Table S4**) thus indicating selection. Selection during soil colonization is
227 also manifested in the variation between biological replicas ($\overline{SD}$ values) of alleles
228 that were enriched in root populations being on average 20 % smaller than those
229 that were not (**Fig. 4d**). Finally, stop codons were purged in all biofilms and soil
230 populations, indicating, as expected, that GudB's activity is required for *B.*
231 *subtilis'* survival under these conditions [22,23].

232 Altogether, as expected [11], in biofilms, and particularly in soil colonization,
233 both drift and selection determine the fate of GudB alleles. The drivers of drift in
234 biofilms were further unraveled as described in the next section.

235

236 **Drift in biofilms is driven by programmed prophage excisions**

237 Mutagenic rates in biofilms are high and mutations with a selective advantage
238 rapidly take over (genetic sweeps) [31]. Growth in biofilms is also spatially defined,
239 giving rise to segregated lineages whereby an entire segment of the biofilm's
240 edge stems from a single cell in which a beneficial mutation had first emerged [11].
241 GudB mutations that happen to be in these 'founder' cells might therefore fixate
242 along these lineages. To examine this hypothesis, we sequenced samples for
243 which enough genomic DNA was available (6 ordinary and 12 gradient biofilms,
244 and for comparison, 2 Initial Mixes, 6 liquid and 4 pellicle samples). A range of
245 single nucleotide polymorphisms (SNPs) in various loci was identified across
246 these samples (**Data S3**). We focused, however, on identifying genomic
247 mutations that were not, or scarcely observed in the Initial Mix and/or in liquid
248 samples and were thus emerged and enriched in the biofilms.

249 Foremost, we observed two large genome deletions that occurred in all
250 biofilms with a frequency approaching 100% (**Figs. 5a** & **5b**). These deletions
251 correspond to the excision of two mobile genetic elements, or prophages, *skin*
252 and SP-β [32–34]. Excision of *skin* generates a functional protein: sigK - a
253 sporulation-specific transcription factor essential for cell differentiation in *B.*
254 *subtilis* [35]. The excision of SP-β generates a functional CapD – an enzyme
255 mediating production of poly-γ-glutamate, an essential component in capsule
256 formation and biofilm development [36,37]. Nearly all biofilm cells carried one of
257 these variations, and most cells carried both (**Fig. 5a & b**; **Table S5** & **Data S3**).
258 Given their dominance [38], these structural variations are likely to be the primary
259 cause of genetic sweeps and of GudB's drift (**Fig. 5c**). These prophage excisions

260 are also likely to occur in the soil, but the DNA recovered from these samples
261 was insufficient to allow genome sequencing.

262 Exclusively in biofilms, we also detected 59 enriched SNPs in a conserved
263 region of 16S rRNA (**Table S5** & **Data S3**). However, *B. subtilis* has ten 16S rRNA
264 gene copies. Since these are essentially identical, we could not determine which
265 of these 10 paralogues carried mutations. However, per population, 98% of the
266 16S rRNA mutations occurred in the same Illumina read suggesting that one
267 paralogue was highly mutated while others remained intact (**Fig. S6**). At this
268 stage, the mechanism of inactivation by multiple proximal 16S mutations, and
269 how inactivation affects biofilm development, remains unclear. Large differences
270 in expression levels of 16S rRNA genes were identified *in P. aeruginosa* biofilms
271 [39], and ribosomal heterogeneity has been linked to biofilm development in *B.*
272 *subtilis* [40]. However, to our knowledge, mutations in the 16S rRNA genes have not
273 been reported in biofilms.

274 Overall, the 16S rRNA SNPs, and the structural variations in particular,
275 seem to have a key role in biofilm development in *B. subtilis*. Accordingly, most of
276 these genetic variations were reproducible between replica experiments (**Table**
277 **S5**) suggesting that they arose during biofilm growth, and then enriched due to
278 their adaptive potential [11]. Thus, although selection dictated the fate of GudB
279 mutations in the early stages of biofilm development, once biofilm promoting
280 mutations appeared and rapidly took over, they drove the fixation of any GudB
281 that happened to be present in the mutated cell.

282

283 **Concluding remarks**

284 Pleiotropy of mutations is assumed but not at the magnitude unraveled here.
285 Environmental changes, including minute ones like addition of arginine to a
286 proline medium, completely revert the effect of up to 84% of the tested GudB
287 mutations. Pleiotropy severely restricts protein sequence space –if all tested
288 conditions are considered, only 2% of the tested GudB mutations are neutral in
289 the 9 reproducible conditions -when selection strongly acts on GudB. This
290 suggests that wild-type GudB's sequence is in fact unique in being shaped under
291 multiple constrains and environments, as also indicated by its dominance in
292 many conditions. Together, pleiotropy and drift dictate the evolution of short-
293 term polymorphism (micro-evolution), but also the evolution of protein
294 sequences along long evolutionary times and across species (macro-evolution).
295 The correlation between the effects of mutations in laboratory mappings under
296 one specific condition and the natural sequence diversity is therefore limited [12].
297 Merging of data from multiple reproducible conditions does not seem to improve
298 correlation, also when applying a number of machine learning techniques
299 (stochastic gradient descent classifier, support vector machines, or random
300 forest classifier; **Fig. S7**).

301 Thus, along short evolutionary periods, proteins experience variable and
302 opposing selection pressures. Additionally, drift may lead to rapid fixation of
303 alleles that are marginally fit or even deleterious. The effects of drift have been
304 extensively studied initiated by Kimura's neutral theory [10]. Our results quantify
305 its effects in bacterial populations and the potential effect of drift in combination
306 with selection across different environments. For example, nearly 80% of the
307 tested mutations survived or enriched sporulation, and a single spore can start a
308 whole new population. However, once the environment changes, such alleles will

be rapidly lost unless compensated by other mutations. Indeed, along macro-evolutionary time scales, epistasis dominates gene and genome sequences [41].

312 **References**

313 1. Baba, T. *et al.* Construction of Escherichia coli K-12 in-frame, single-gene
314 knockout mutants: The Keio collection. *Mol. Syst. Biol.* **2,** (2006).
315 2. Koo, B. M. *et al.* Construction and Analysis of Two Genome-Scale Deletion
316 Libraries for Bacillus subtilis. *Cell Syst.* **4,** 291–305.e7 (2017).
317 3. Pache, R. A., Madan, M. M. & Aloy, P. Exploiting gene deletion fitness effects
318 in yeast to understand the modular architecture of protein complexes
319 under different growth conditions. *BMC Syst. Biol.* **3,** (2009).
320 4. Winzeler, E. A. *et al.* Functional characterization of the S. cerevisiae
321 genome by gene deletion and parallel analysis. *Science (80-.).* **285,** 901–
322 906 (1999).
323 5. Civelek, M. & Lusis, A. J. Systems genetics approaches to understand
324 complex traits. *Nature Reviews Genetics* **15,** 34–48 (2014).
325 6. Steinberg, B. & Ostermeier, M. Environmental changes bridge evolutionary
326 valleys. *Sci. Adv.* **2,** e1500921 (2016).
327 7. Fusco, D., Gralka, M., Kayser, J., Anderson, A. & Hallatschek, O. Excess of
328 mutational jackpot events in expanding populations revealed by spatial
329 Luria-Delbrück experiments. *Nat. Commun.* **7,** (2016).
330 8. Kimura, M. Genetic variability maintained in a finite population due to
331 mutational production of neutral and nearly neutral isoalleles. *Genet. Res.*
332 *(Camb).* **89,** 341–363 (2008).
333 9. Smith, N. H., Gordon, S. V., de la Rua-Domenech, R., Clifton-Hadley, R. S. &
334 Hewinson, R. G. Bottlenecks and broomsticks: The molecular evolution of
335 Mycobacterium bovis. *Nature Reviews Microbiology* **4,** 670–681 (2006).
336 10. Nei, M. Selectionism and neutralism in molecular evolution. *Molecular*
337 *Biology and Evolution* **22,** 2318–2342 (2005).
338 11. Steenackers, H. P., Parijs, I., Foster, K. R. & Vanderleyden, J. Experimental
339 evolution in biofilm populations. *FEMS Microbiology Reviews* **40,** 373–397
340 (2016).
341 12. Boucher, J. I., Bolon, D. N. A. & Tawfik, D. S. Quantifying and understanding
342 the fitness effects of protein mutations: Laboratory versus nature. *Protein*
343 *Science* 1219–1226 (2016). doi:10.1002/pro.2928
344 13. De Visser, J. A. G. M. & Krug, J. Empirical fitness landscapes and the
345 predictability of evolution. *Nature Reviews Genetics* **15,** 480–490 (2014).
346 14. Fowler, D. M. & Fields, S. Deep mutational scanning: A new style of protein
347 science. *Nature Methods* **11,** 801–807 (2014).
348 15. Steinberg, B. & Ostermeier, M. Shifting Fitness and Epistatic Landscapes
349 Reflect Trade-offs along an Evolutionary Pathway. *J. Mol. Biol.* **428,** 2730–
350 2743 (2016).
351 16. Dandage, R., Pandey, R., Jayaraj, G. & Chakraborty, K. Differential Strengths
352 Of Molecular Determinants Guide Environment Specific Mutational Fates.
353 *biorxiv* (2017). doi:10.1101/134569
354 17. Earl, A. M., Losick, R. & Kolter, R. Ecology and genomics of Bacillus subtilis.
355 *Trends in Microbiology* **16,** 269–275 (2008).
356 18. Vlamakis, H., Chai, Y., Beauregard, P., Losick, R. & Kolter, R. Sticking
357 together: Building a biofilm the Bacillus subtilis way. *Nature Reviews*
358 *Microbiology* **11,** 157–168 (2013).
359 19. Branda, S. S., González-Pastor, J. E., Ben-Yehuda, S., Losick, R. & Kolter, R.

360 Fruiting body formation by Bacillus subtilis. *Proc. Natl. Acad. Sci. U. S. A.*
361 **98,** 11621–6 (2001).
362 20. Belitsky, B. R. & Sonenshein, A. L. Role and regulation of Bacillus subtilis
363 glutamate dehydrogenase genes. *J. Bacteriol.* **180,** 6298–305 (1998).
364 21. Gunka, K. & Commichau, F. M. Control of glutamate homeostasis in Bacillus
365 subtilis: A complex interplay between ammonium assimilation, glutamate
366 biosynthesis and degradation. *Molecular Microbiology* **85,** 213–224
367 (2012).
368 22. Liu, J. *et al.* Metabolic co-dependence gives rise to collective oscillations
369 within biofilms. *Nature* **523,** 550–554 (2015).
370 23. Noda-Garcia, L., Romero Romero, M. L., Longo, L. M., Kolodkin-Gal, I. &
371 Tawfik, D. S. *Bacilli* glutamate dehydrogenases diverged via coevolution of
372 transcription and enzyme regulation. *EMBO Rep.* **18,** 1139–1149 (2017).
373 24. De Jong, L. *et al.* In-Culture Cross-Linking of Bacterial Cells Reveals Large-
374 Scale Dynamic Protein-Protein Interactions at the Peptide Level. *J.*
375 *Proteome Res.* **16,** 2457–2471 (2017).
376 25. Stannek, L. *et al.* Evidence for synergistic control of glutamate biosynthesis
377 by glutamate dehydrogenases and glutamate in Bacillus subtilis. *Environ.*
378 *Microbiol.* **17,** 3379–3390 (2015).
379 26. Belogurov, G. A. & Artsimovitch, I. Regulation of Transcript Elongation.
380 *Annu. Rev. Microbiol.* **69,** 49–69 (2015).
381 27. Kobayashi, K. *et al.* Essential Bacillus subtilis genes. *Proc. Natl. Acad. Sci.*
382 **100,** 4678–4683 (2003).
383 28. Mondal, S., Yakhnin, A. V., Sebastian, A., Albert, I. & Babitzke, P. NusA-
384 dependent transcription termination prevents misregulation of global
385 gene expression. *Nat. Microbiol.* **1,** (2016).
386 29. Besharova, O., Suchanek, V. M., Hartmann, R., Drescher, K. & Sourjik, V.
387 Diversification of gene expression during formation of static submerged
388 biofilms by Escherichia coli. *Front. Microbiol.* **7,** (2016).
389 30. Mavor, D. *et al.* Determination of ubiquitin fitness landscapes under
390 different chemical stresses in a classroom setting. *Elife* **5,** (2016).
391 31. Nguyen, D. & Singh, P. K. Evolving stealth: genetic adaptation of
392 Pseudomonas aeruginosa during cystic fibrosis infections. *Proc. Natl. Acad.*
393 *Sci. U. S. A.* **103,** 8305–8306 (2006).
394 32. Kunkel, B., Losick, R. & Stragier, P. The Bacillus subtilis gene for the
395 developmental transcription factor σ(K) is generated by excision of a
396 dispensable DNA element containing a sporulation recombinase gene.
397 *Genes Dev.* **4,** 525–535 (1990).
398 33. Nicolas, P. *et al.* Condition-dependent transcriptome reveals high-level
399 regulatory architecture in Bacillus subtilis. *Science (80-.).* **335,** 1103–1106
400 (2012).
401 34. Westers, H. *et al.* Genome Engineering Reveals Large Dispensable Regions
402 in Bacillus subtilis. *Mol. Biol. Evol.* **20,** 2076–2090 (2003).
403 35. Eichenberger, P. *et al.* The program of gene transcription for a single
404 differentiating cell type during sporulation in Bacillus subtilis. *PLoS Biol.* **2,**
405 (2004).
406 36. Abe, K. *et al.* Developmentally-Regulated Excision of the SPβ Prophage
407 Reconstitutes a Gene Required for Spore Envelope Maturation in Bacillus
408 subtilis. *PLoS Genet.* **10,** (2014).

37. Davey, M. E. & Duncan, M. J. Enhanced biofilm formation and loss of capsule synthesis: Deletion of a putative glycosyltransferase in Porphyromonas gingivalis. *J. Bacteriol.* **188,** 5510–5523 (2006).
38. Martin, M. *et al.* De novo evolved interference competition promotes the spread of biofilm defectors. *Nat. Commun.* **8,** (2017).
39. Pérez-Osorio, A. C., Williamson, K. S. & Franklin, M. J. Heterogeneous rpoS and rhlR mRNA levels and 16S rRNA/rDNA (rRNA Gene) ratios within Pseudomonas aeruginosa biofilms, sampled by laser capture microdissection. *J. Bacteriol.* **192,** 2991–3000 (2010).
40. Vesper, O. *et al.* Selective translation of leaderless mRNAs by specialized ribosomes generated by MazF in Escherichia coli. *Cell* **147,** 147–157 (2011).
41. Breen, M. S., Kemena, C., Vlasov, P. K., Notredame, C. & Kondrashov, F. A. Epistasis as the primary factor in molecular evolution. *Nature* **490,** 535–538 (2012).
42. Konkol, M. A., Blair, K. M. & Kearns, D. B. Plasmid-encoded comi inhibits competence in the ancestral 3610 strain of Bacillus subtilis. *J. Bacteriol.* **195,** 4085–4093 (2013).
43. Yi, Y., de Jong, A., Frenzel, E. & Kuipers, O. P. Comparative transcriptomics of Bacillus mycoides root exudates reveals different genetic adaptation of endophytic and soil isolates. *Front. Microbiol.* **8,** (2017).
44. Deatherage, D. E. & Barrick, J. E. Identification of mutations in laboratory-evolved microbes from next-generation sequencing data using breseq. *Methods Mol. Biol.* **1151,** 165–188 (2014).

Acknowledgments

L.N.G. was supported by the CONACYT grant #203740 and the Martin Kushner Fellowship at the Weizmann Institute of Science. D.S.T. is the Nella and Leon Benoziyo Professor of Biochemistry. Financial support by the Kahn Center for Systems Biology at the Weizmann Institute of Science is gratefully acknowledged. We are highly grateful to Ron Milo, Sarel Fleishman, Zvi Livneh and Fyodor Kondrashov for support and critical advice, to Einat Segev, Arjan de Visser for critical and insightful comments to the manuscript. We highly appreciate the help of Moshe Hershko in script development for data processing. We are thankful for the services provided by the Crown Genomics institute of the

Nancy and Stephen Grand Israel National Center for Personalized Medicine, Weizmann Institute of Science.

Authors Contribution

L.N.G. and D.S.T. designed experiments and wrote the manuscript. L.N.G., D.D. and D.S.T. analysed the data. L.N.G. performed all experiments, except selection in soil colonization that was performed in collaboration with E.K. and A.A. D.D. and A.E. wrote the scripts used for data analysis and visualization. E.P. applied machine learning classification.

454 **Fig. 1. Selection *versus* chance-dominated conditions. (A)** Dot-plot indicating
455 reproducible measurements of frequency coefficients of individual mutations
456 (FC values) in three parallel replica liquid cultures with proline as carbon-
457 nitrogen source. $\overline{SD}$ is the average standard deviation between biological
458 replicas. The S.D. values were calculated per each amino acid allele based on
459 logFC values and averaged for all alleles in a given condition. **(B)** The same
460 analysis of three parallel biofilms with arginine as carbon-nitrogen source
461 indicates low reproducibility. **(C)** The $\overline{SD}$ values categorized by the 7 general
462 growth states tested here. Each point represents the $\overline{SD}$ value between replicas
463 of the same experiment (the distributions of SD values per each condition are
464 shown in **Fig. S3a**). **(D)** $\overline{SD}$syn represents the standard deviation between the
465 logFC values of synonymous codons. The standard deviations per allele were
466 averaged for all synonymous alleles in the same replica experiment, and then
467 averaged across the 3 replica experiments in a given condition (the distributions
468 of SD*syn* values per experiment are shown in **Fig. S3b**).
469

470 **Fig. 2. The pleiotropic effects of alleles across different conditions.** (**A**) A
471 dot-blot correlation of FC values of individual alleles in three different liquid
472 carbon-nitrogen sources. The red squares encompass alleles that show sign
473 pleiotropy – i.e., a change from beneficial to deleterious, or vice versa. (**B**)
474 Pairwise correlation of the FC values in all 9 different reproducible conditions
475 (average FC values of all alleles and replicas). Colors indicate the Pearson
476 correlation values (-1, negative correlation; 0, no correlation; 1, positive
477 correlation). The strongest anti-correlation was found with arginine as carbon-
478 nitrogen source (black square). **(C)** The distribution of alleles by their level of
479 sign pleiotropy. From pale to dark): (*i*) Weak sign pleiotropy (changes between
480 deleterious and beneficial); (*ii*) Mild sign pleiotropy (changes from highly
481 deleterious to beneficial, or from highly beneficial to deleterious); and (*iii*)
482 Strong sign pleiotropy (changes from highly deleterious to highly beneficial, or
483 vice versa). The fraction of alleles showing mild or strong sign pleiotropy is
484 shown above the bars. The control dataset comprises 4 completely independent
485 growth experiments in liquid proline, each inoculated from a different initial mix
486 and grown on separate occasions (**Fig. S8**). Nonetheless, none of the alleles in
487 this control set exhibited strong pleiotropy.
488

489 **Fig. 3. Genetic sweeps in biofilms and soil.** Photographs of: **(A)** normal
490 biofilms; **(B)** gradient biofilms; **(C)** a scheme of soil colonization (shown biofilms
491 with proline as carbon-nitrogen source). **(D)** The distribution of frequency of
492 individual alleles for different growth states with proline as carbon-nitrogen
493 source. Bar widths represent allele frequency from raw read counts (Rf values**;**
494 **Data S1**). Magenta corresponds to wild type GudB. **(E)** Alleles with Rf ≥ 1% were
495 identified and their number and sum of frequencies are shown (averages and
496 standard deviations for all experiments in a given condition). Blue designates
497 selection-dominated conditions and red drift-dominated ones, as in **Fig. 1**.
498

Fig. 4. The combined action of selection and chance in biofilms (red) and soil colonization (green). (A) Alleles that enriched in the edge of the biofilms are more likely to arise from alleles that were neutral or enriched in the center. The distribution of categorized FC values from all biofilm centers (grey) compared to the distribution of FC values of center alleles that were enriched in the edge (red). **(B)** The distribution of categorized FC values of all alleles in all liquid conditions (grey) compared to the distribution of FC values of liquid alleles that were enriched in the edge of biofilms (red). **(C)** Alleles enriched in the root are more likely to arise from alleles that were enriched in the bulk soil. The distribution of categorized allele FC values in all soil samples (grey) compared to the distribution of FC values of soil alleles that were enriched in the root (green). T-tests were computed per each FC category. One, two or three asterisks indicate a p-value < 0.05, <0.001, or < 0.005, respectively. **(D)** The distribution of SD values (variability between replica experiments, as in **Fig. 1c**) of alleles enriched in one or more root populations compared to alleles that were never enriched in the roots.

516 **Fig. 5. Programmed genomic excisions drive GudB's drift in biofilms.**
517 Schematic representation of *B. subtilis* genomic organization before and after the
518 excision of the prophage mobile elements SP-β (**A**) and *skin* (**B**) and their
519 position in the genome. (**C**) These excisions were absent in the initial mix yet
520 dominated biofilms and went to near fixation in the edge of gradient biofilms (for
521 frequencies in individual experiments see **Table S5**). Excision of the mobile
522 elements occurred in two different genomic locations within the same
523 experiment. The values were summed and averaged according to the general
524 condition shown. The details of the excisions (location and frequency) per
525 experiment are shown in **Data S3**.
526

527 **Materials and Methods**

528 **Strains**

529 *B. subtilis* NCIB 3610 DS7187 (gently gifted by Dr. Daniel B. Kearns [42]) that lacks
530 the ComI peptide and has high competence capacity similar to domesticated *B.*
531 *subtilis* strains was recruited to this study. *Bacillus subtilis* NCIB 3610 *gudB::tet*
532 strain [23] genomic DNA was transformed into *B. subtilis* NCIB 3610 DS7187. *B.*
533 *subtilis* NCIB 3610 *ΔcomI gudB::tet* was thus isolated, and was phenotypically
534 and genetically tested.

535

536 **GudB allele library construction**

537 We performed site directed mutagenesis in 10 codons (amino acids: M46, L48,
538 K52, D58, D59, S61, K63, T66, Y68, S75) of the *gudB* gene cloned in the
539 pDG_GudB plasmid [23]. The codons were mutated to NNS (N = all bases & S = C or
540 G) whereby the 20 standard amino acids and 1 stop codon is encoded. The codon
541 mutagenesis was done in one step PCR protocol and independently for each
542 position. Thus, we created 10 libraries, each containing 20 different amino acid
543 alleles (non-synonymous, missense mutations), 1 stop-codon (nonsense), and 11
544 synonymous alleles (alternative codons encoding the same amino acid). All
545 mutagenic PCRs were performed with Kapa HiFi HotStart Ready Mix (Kapa
546 Biosystems) following manufacturers conditions (**Table S6** shows the sequence
547 of all primers). The 10 PCR products were purified and used to transform the *E.*
548 *coli* T10 strain (Thermo Fisher Scientific). Clones were pulled together after an
549 overnight growth on LB + Ampicillin (100 μg/ml) agar plates at 37°C. At this
550 stage, 4 to 6 clones per library were isolated and analyzed by sequencing. Total
551 plasmid DNA from these library transformations was extracted and also
552 analyzed by sequencing. Each of the 10 libraries contained, after transformation,
553 at least 10^5 clones, corresponding to ≥ 1000-fold coverage per allele.
554 Approximately 10 μg of plasmid DNA, from each library, was linearized (XhoI,
555 New England Biolabs, following manufactures conditions), purified, and used to
556 transform the *B. subtilis* NCIB 3610 *gudB::tet ΔcomI* strain. Transformations were
557 performed as described [23]. After transformation, overnight growth on in +
558 Spectinomycin (100μg/ml) + Glucose (0.5 mg/ml) agar plates was used as
559 selection. The resulting cells were pulled together and kept at -20°C in 50%

560 glycerol. In total, 10 *B. subtilis* libraries were constructed in parallel and each
561 contained, after transformation, at least 10^4 clones (≥100-fold coverage per
562 allele). Genomic DNA extraction of each library was performed (GenElute -
563 Sigma). The integrity of the mutagenic process was verified by sanger
564 sequencing the *amyE::gudB* locus indicating that mutations were observed only
565 in the diversified codon.
566
567 **Selection and growth conditions**
568 10 ml of LB with Glucose (0.5%), ammonium sulfate (0.5%) and spectinomycin
569 (100 µg/ml) cultures were inoculated with 1 ml of each library stock. The
570 cultures were grown overnight at 37°C with shaking. 500 µl of the overnight
571 culture was used to inoculate 3 ml of LB plus glucose (0.5%) and ammonium
572 sulfate (0.5%). The cultures were incubated at 37°C with shaking and once the
573 $O.D._{600}$ reached 0.8 they were mixed equally and used as the starting population
574 (Initial Mix). A fraction of the cells at this stage were harvested by centrifugation
575 and stored for genomic DNA purification. In total, three different initial mixes
576 were used for the experiments described here. Initial Mix #1 was used to
577 inoculate most liquid conditions (4 carbon-nitrogen sources), pellicles and
578 gradient biofilms. Initial Mix #2 was used to inoculate 1 liquid condition, spores,
579 germination and biofilms, and Initial Mix #3 was used to inoculate bulk soil
580 (**Data S1**). Detailed selection conditions are listed below:
581 For selection under liquid serial passages 100 ul of the Initial Mix was used to
582 inoculate 10 ml cultures of MS medium [23] with glucose (0.5%) plus ammonium
583 sulfate (0.5%), glutamate (0.5%) plus glycerol (0.5%), proline (0.5%), arginine
584 (0.5%) or proline (0.25%) plus arginine (0.25%). The cultures were incubated at
585 37°C with shaking until $O.D._{600}$ reached 1 – 1.5, after which 100 µl was used to
586 inoculate 10 mL of fresh medium. The serial passages were done every 24 hours
587 when proline (0.5%), arginine (0.5%) or proline (0.25%) plus arginine (0.25%)
588 where used as carbon-nitrogen sources, and every 12 hours when glucose
589 (0.5%) plus ammonium sulfate (0.5%), or Glutamate (0.5%) plus glycerol
590 (0.5%), were applied. In total, all liquid passages were maintained for
591 approximately 50 generations.

592 For selection in pellicles, 100 ml of media (b), (c) and (d) were inoculated with
593 100 µl of the initial mix cells. The culture was incubated at 30°C without shaking,
594 for 5 days.
595 For selection of spores and germinated spores, three ml of the Initial Mix was
596 used to inoculate 25 ml of Difco Sporulation Medium (DSM) in 250 ml flasks and
597 incubated at 37°C with 150 rpm shaking until O.D.600 reached 0.4. This culture
598 was used to inoculate 250 ml of fresh DSM in 1L flasks. The cultures were
599 incubated 48h at 37°C with 150 rpm shaking. Cells were subsequently harvested
600 by centrifugation and stored at 4°C over night. After, cells were re-suspended
601 with 200 ml of cold deionized sterile water (dW) and incubated for 30 min at
602 4°C. Cells were harvested and re-suspended with 200 ml of cold distilled water
603 (dW) and incubated overnight at 4°C with slow orbital agitation, to kill all
604 planktonic of vegetative cells. The culture was harvested, re-suspended in 30 ml
605 of dW and heated to 80°C for 20 min. Finally, spores were harvested, re-
606 suspended in 10 ml of dW, and stored at -20°C. To germinate these spores, they
607 were diluted 1000 times in phosphate-buffered saline solution and 100 µl of this
608 suspension was used to inoculate LB plus glucose (0.5%) agar plates (10 plates).
609 Approximately 10,000 colonies were obtained and pulled together.
610 For selection in biofilms, MS agar (1.5%) plates supplemented with different
611 carbon-nitrogen sources were prepared. For gradient biofilms, gradient agar
612 plates were prepared. First, square plates (12x12 cm) with MS agar (1.5%)
613 medium were poured. After the agar solidified, an area of 2x14 cm was removed
614 from the top of the plate. In this area, a solution of either Proline 5%, Arginine
615 5%, monosodium glutamate 5% or Glycerol 5% in 1.5% agar was poured into
616 the removed section. For the glutamate plus glycerol gradient biofilm, two
617 opposite areas of the agar plate were removed. Into one, a solution of
618 monosodium glutamate (5%) in 1.5% agar was poured, and into the other,
619 glycerol (5%) plus 1.5% agar solution (see **Fig. S9a** for a graphic representation
620 of the agar plates preparation). All gradient agar plates were incubated for 24 h
621 at room temperature before use. We also calibrated the place in the gradient
622 plate where we inoculated the cells such that we observed growth after 1 night
623 incubation at 30°C (**Fig. S9b**). For growth in biofilms and gradient biofilms, 5 µl
624 of the Initial Mix were used as inoculum. Plates were incubated for 4 days at

625 30°C and 2 more days at room temperature. The colony was then dissected in 3
626 areas (center, wrinkle and edge) for normal biofilms, and in 2 areas (center and
627 upper) for gradient biofilms (illustrated in **Fig. S9c-g**). After selection in all the
628 above-mentioned conditions the biomass was harvested and storage at -20°C. All
629 growth experiments were performed in triplicate by inoculating with the same
630 Initial Mix.
631 For selection in soil and plant roots, the Initial Mix was generated as above-
632 mentioned except that the process was scaled up (instead of 3 ml, 10 ml of
633 culture was prepared per library). In total, 200 ml of the Initial Mix ($O.D._{600}$ = 0.8)
634 was applied. This LB culture was washed three times (by means of centrifugation
635 and re-suspension) with 100 ml half strength Hoagland solution [43]. Since
636 Hoagland's solution is not isotonic, the washes resulted in death of about a third
637 of the *B. subtilis* cells. Thus, handling the samples at this stage was performed as
638 fast as possible. After the final wash, the cells were re-suspended in half strength
639 Hoagland solution to a final $O.D._{600}$ of 0.1. Natural soil was collected at the Ha-
640 Masrek Reserve, Israel (31.793 N, 35.042 E), sifted through 2 mm sieve and
641 autoclaved three times for 30 min at 121°C. A total of five pots (size 10 x 8 x 5
642 cm) with autoclaved natural soil were drenched with the Initial Mix suspended
643 in half strength Hoagland Solution [43]. These potted soils drenched with bacterial
644 suspensions were used to plant tomato seedlings grown first in sterile
645 conditions. Seeds of tomato (*Solanum lycopersicum L.*; cv. Micro-Tom) were
646 surface-sterilized with 70% ethanol for 5 minutes and, 10 minutes with 3%
647 bleach with 0.01% Tween 20. Surface-sterile seeds were germinated on sterile
648 filter paper (Whatman, catalog # 1001-085) saturated with half strength
649 Hoagland Solution for 7 days (23°C and 16 hours photoperiod). Six tomato
650 seedlings were transferred to each pot and grown for one month (21°C, 16h
651 light, 8h dark) with drenching with half strength Hoagland twice a week. Plants
652 were subsequently harvested from the five pots. Roots and rhizosphere samples
653 were collected for each replica experiment consisting a pool of six roots. First,
654 the plants were carefully removed from the soil. Roots were then cut out from
655 the plants and vortexed in 20 ml of washing solution (0.85% NaCl) for 30 s. This
656 step was repeated one more time with a fresh washing solution. The combined
657 root washing solutions (40 ml) was centrifuged for 30 min at 3000 rpm and the

658 resulted pelleted samples corresponding to the rhizosphere were frozen in liquid
659 nitrogen and stored at -80°C. The washed roots were blotted in filter paper and
660 stored at −80°C until further use. Finally, bulk soil without roots was also stored
661 at −80°C.
662
663 **Genomic DNA extraction**
664 All samples, including pellicle, spores, biofilm and gradient biofilm samples, were
665 defrosted and re-suspended in 10 ml of dW. The samples were sonicated at 40%
666 power, VibraCell, Sonics, for 10 min at 60 s intervals. Cells debris was harvested
667 by centrifugation (13,000 g for 20 min). Genomic DNA from all samples was
668 extracted using the GenElute Bacterial Genomic DNA Kit (Sigma-Aldrich)
669 generally following the manufacturer's instructions, with the exception of the
670 soil, rhizosphere soil and plant roots samples. For these samples, the PowerSoil
671 DNA Isolation kit of Mo Bio was used, following its manufacturer's instructions.
672
673 **Illumina sample preparations**
674 The mutagenized *gudB* fragment (from amino acids 45 to 81) was amplified
675 using the primers GudB_In_For (5'-
676 CTCTTTCCCTACACGACGCTCTTCCGATCTnnnnnnCCCGAAGAGGTATACGAATTGT
677 TAAAAGAG), and GudB_In_Rev (5'-
678 CTGGAGTTCAGACGTGTGCTCTTCCGATCTCGCCTTTCGTTGGACCGAC). To the
679 GudB_In_For primer, 6 N's were added to increase the sequence variability
680 between amplicons. PCRs were performed with the KapaHiFi HotStart Ready Mix
681 (Kapa Biosystems) using approximately 100 ng of genomic DNA as template and
682 following manufacturer's instructions. Using 10 µl of the PCR as template, a
683 second PCR was performed to add the Illumina adaptor sequence, using primers
684 GudB_Out_For (5'-
685 AATGATACGGCGACCACCGAGATCTACACTCTTTCCCTACACGACGC) and
686 GudB_Out_Rev (5'-
687 CAAGCAGAAGACGGCATACGAGAT<u>TGTTATAC</u>GTGACTGGAGTTCAGACGTGTGC).
688 The Illumina index (underlined) was changed in the GudB_Out_Rev primer to
689 different Illumina indexes. Each condition was differently barcoded. All PCRs
690 were purified using the Agencourt AMPure XP (Beckman Coulter). The

concentration of PCR products was verified using Qu-bit assay (Life Technologies).

Analysis of the Illumina reads

DNA samples were run using the Illumina NextSeq 150-bp paired-end kit. The FASTQ sequence files were obtained for each run and customized using MatLab 8.0 and Python 3.6 scripts designed to count the number of each individual allele in each sequenced sample. We filtered the reads to exclude any reads that have mutations outside the mutagenized codons. All codons encoding for the wild-type amino acid were summed in one and assigned as WT. All other codons were counted independently. The unprocessed read counts are shown in **Data S1**. Further filtering excluded alleles with < 100 counts in the Initial mix to avoid statistical uncertainty with respect to FC values. In total, we obtained data for up to 269 individual alleles per condition out of the originally introduced 320 alleles. Per condition, a minimum of 380,000 reads was obtained. Thus, in average, we obtained 1500 reads per allele.

Data Analysis

The frequency of each allele (f_i) was calculated as the ratio between the number of reads for allele i divided by the total number of reads. The allele frequency coefficient (FC_i) was subsequently calculated as the ratio of after selection (f_i) divided by the frequency of the same allele in the initial mix (**Fig. S2** & **Data S2**). Normalization by the number of wild-type reads rather than by the total number of reads gave essentially identical FC values for the majority of samples. However, in the few samples where wild-type frequency was significantly reduced after selection, normalization by wild-type reads resulted in high noise and large biases including large changes in sign (higher sign pleiotropy). FC values relate to fitness logarithmically, and thus logFC values were compared. To this end, all FC's equal to zero had to be changed, and we opted for a tenth of the minimum FC value found amongst all experiments. For the liquid, pellicles, biofilms, spores and germinated spores experiments (**Data S2, sheet 1**) the zeros were changed to 4.2×10^{-6}. For the bulk soil experiments (**Data S2, sheet 2**) zeros were changed to 1.14×10^{-5}. The logarithm of all FC values was calculated and was also used to derive mean FC values. The logFC values were

724 then used to calculate: (i) the standard deviation for all alleles across conditions
725 ($\overline{SD}$; the standard deviation between logFC values observed per each allele in
726 replica experiments were averaged for all alleles measured in a given condition);
727 (ii) the standard deviation between synonymous codons within the same replica
728 experiment (deviations between logFC values of synonymous codons of the same
729 amino acid allele were calculated, averaged for all alleles in the same experiment,
730 and then for all replica experiments per condition).
731
732 **Defining the limits of neutrality**
733 From all conditions tested here, only in glucose plus ammonia the GudB
734 knockout had no growth effect (**Fig. S1**). Hence, this condition is largely neutral,
735 and the variation observed in FC values would primarily be the outcome of noise.
736 The standard deviation between 3 biological replicas was calculated per allele,
737 and these values spanned over the range of 0.002 to 0.199. We rounded this
738 number to 0.2. Thus, by the strictest measure, FC values between 0.8 and 1.2
739 were classified as 'neutral'. Accordingly, FC ≤0.8 unambiguously assigned a
740 mutation as 'deleterious', and FC >1.2 as 'beneficial'.
741
742 **Genome sequencing**
743 We sequenced the genomic DNA of all biofilm populations for which we had ≥ 1
744 μg of DNA after extraction (6 normal and 12 gradient biofilm). For comparison,
745 we also sequenced Initial mix populations 1 and 2, 6 Liquid and 4 pellicle
746 populations. The Illumina HiSeq2500 platform was used, with 2x125 base pairs
747 read length. We obtained a total of 300 million reads. The reads were assembled
748 using as reference the *B. subtilis* NCIB 3610 genome (NCBI Accession number:
749 CP020102). Overall, 95% of all reads were successfully mapped to the reference
750 genome with minimal coverage of x300 for all samples analyzed. The Breseq
751 program was used to identify genomic variants, including single nucleotide
752 polymorphisms (SNPs) and insertion-deletion polymorphisms (INDELs) [44] (**Data**
753 **S3** & **Table S5**).
754
755 **Comparison of FC values and to GudB's natural sequence variability**

We examined whether the FC values for individual mutations, in individual conditions, might predict whether or not a certain sequence exchange is observed, or not, amongst the sequences of extant GDHs. To this end, we constructed a number of different support vector machines (SVM) classification models with a variety of kernels (such as linear, Gaussian, polynomial etc.). The feature vector of each GudB allele was composed from the normalized FC values from specific condition. The values from replica experiments of the highly reproducible liquid conditions were averaged prior to training. Based on the multiple sequence alignment containing 1013 GDH sequences, we divided the GudB mutations in our dataset into 3 categories, which were then utilized as the prediction labels: (1) mutations seen in less than 5 natural GDH sequences (classified as 'not present', 66% of mutations), (2) mutations observed in 5 - 49 sequences ('rare', 19%) and (3) mutations present in ≥50 sequences ('frequent', 15%). Introducing class weights into the loss function compensated the unbalanced nature of the dataset. For each feature combination of a varied length, we built an SVM classification model and assessed its accuracy using 3-fold cross validation. Additionally, in order to reduce noise, assuming that our data belong to linear space, we extracted the first ten principal components of the feature matrix and used them as the new feature vectors for a model construction. To examine if our relatively high (>0.6) model accuracy was distributed uniformly across different classes, for each model and genotype, we recorded the predicted values during 3-fold cross-validation. Moreover, for each condition combination, and for each kernel, we built 100 different models and recorded the number of times each of the genotypes was predicted correctly.

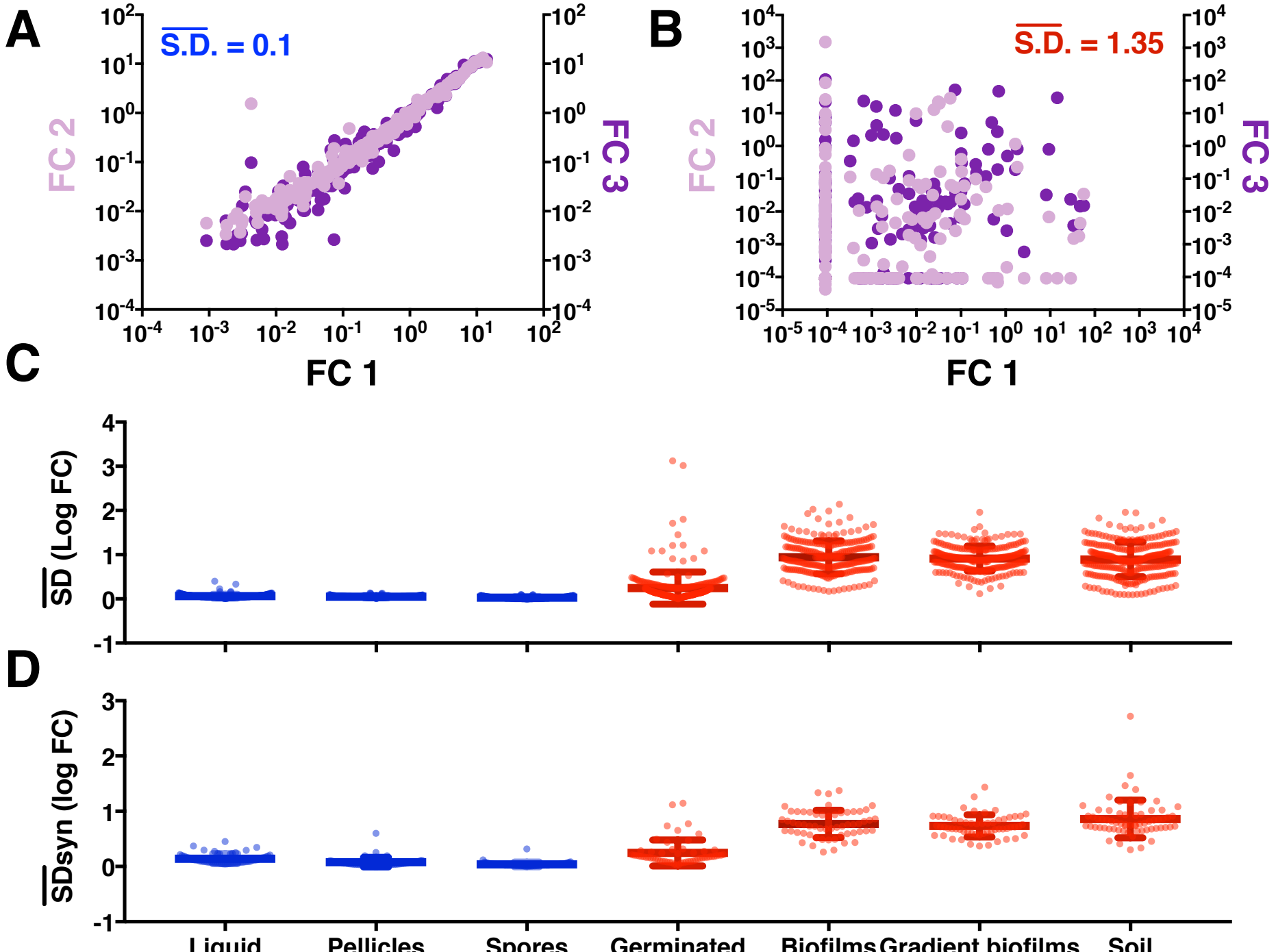
A
S.D. = 0.1
FC 2
FC 3
FC 1
B
S.D. = 1.35
FC 2
FC 3
FC 1
C
SD (Log FC)
D
SDsyn (log FC)
Liquid
Pellicles
Spores
Germinated
Biofilms
Gradient biofilms
Soil

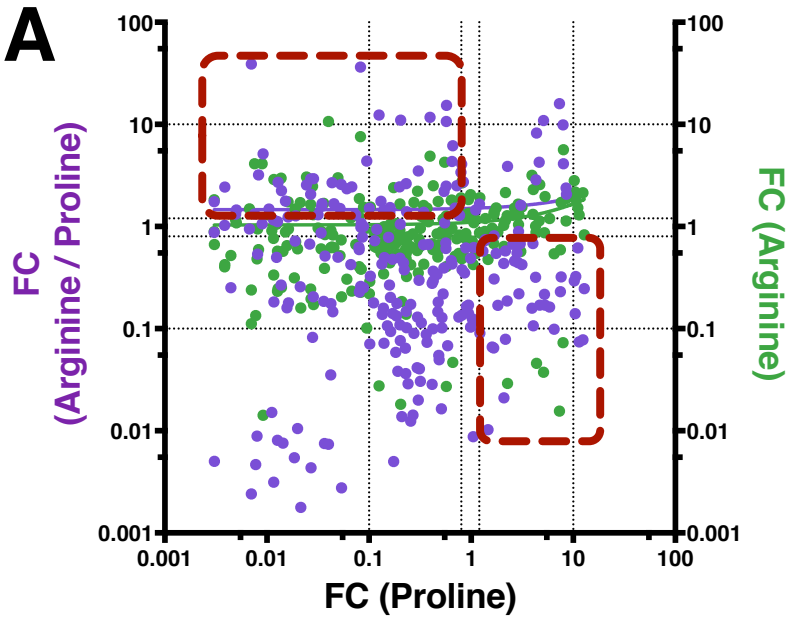
A
FC (Arginine / Proline)
FC (Arginine)
FC (Proline)
100
10
1
0.1
0.01
0.001

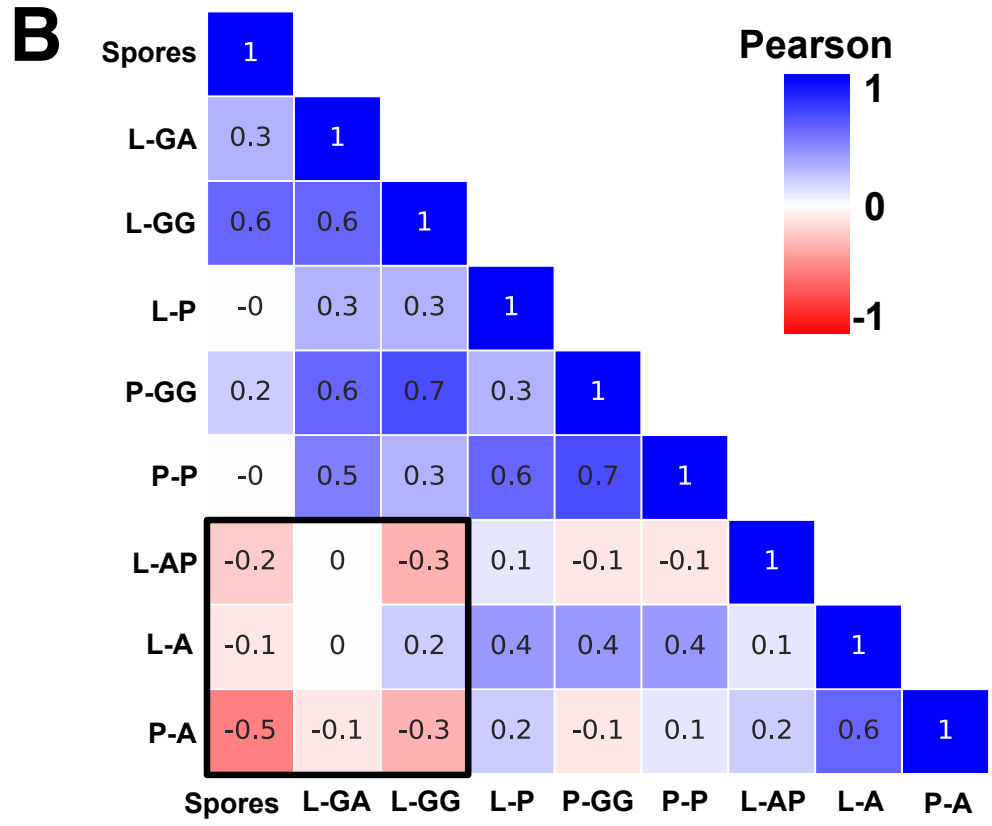
B
Pearson
1
0
-1
Spores 1
L-GA 0.3 1
L-GG 0.6 0.6 1
L-P -0 0.3 0.3 1
P-GG 0.2 0.6 0.7 0.3 1
P-P -0 0.5 0.3 0.6 0.7 1
L-AP -0.2 0 -0.3 0.1 -0.1 -0.1 1
L-A -0.1 0 0.2 0.4 0.4 0.4 0.1 1
P-A -0.5 -0.1 -0.3 0.2 -0.1 0.1 0.2 0.6 1
Spores L-GA L-GG L-P P-GG P-P L-AP L-A P-A

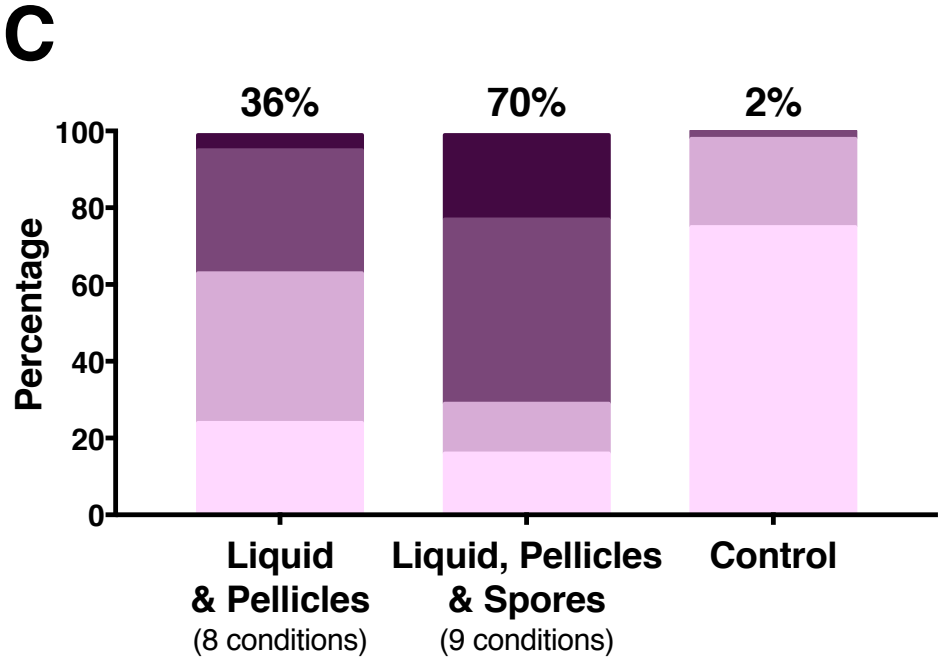
C
36%
70%
2%
Percentage
100
80
60
40
20
0
Liquid & Pellicles
(8 conditions)
Liquid, Pellicles & Spores
(9 conditions)
Control

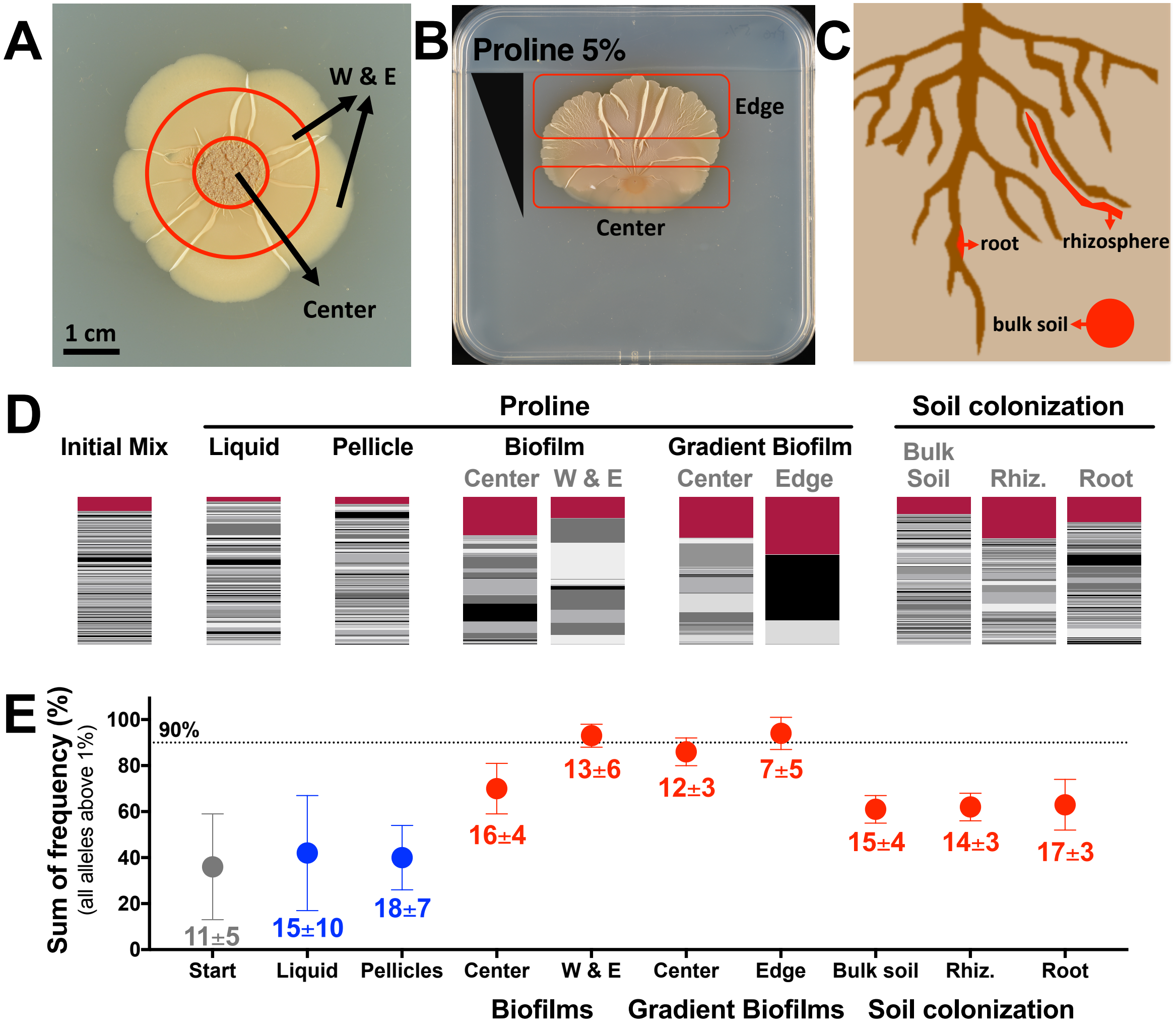
A
W & E
Center
1 cm
B
Proline 5%
Edge
Center
C
root
rhizosphere
bulk soil
D
Proline
Soil colonization
Initial Mix
Liquid
Pellicle
Biofilm
Gradient Biofilm
Center
W & E
Center
Edge
Bulk Soil
Rhiz.
Root
E
Sum of frequency (%)
(all alleles above 1%)
100
80
60
40
20
0
90%
11±5
15±10
18±7
16±4
13±6
12±3
7±5
15±4
14±3
17±3
Start
Liquid
Pellicles
Center
W & E
Center
Edge
Bulk soil
Rhiz.
Root
Biofilms
Gradient Biofilms
Soil colonization

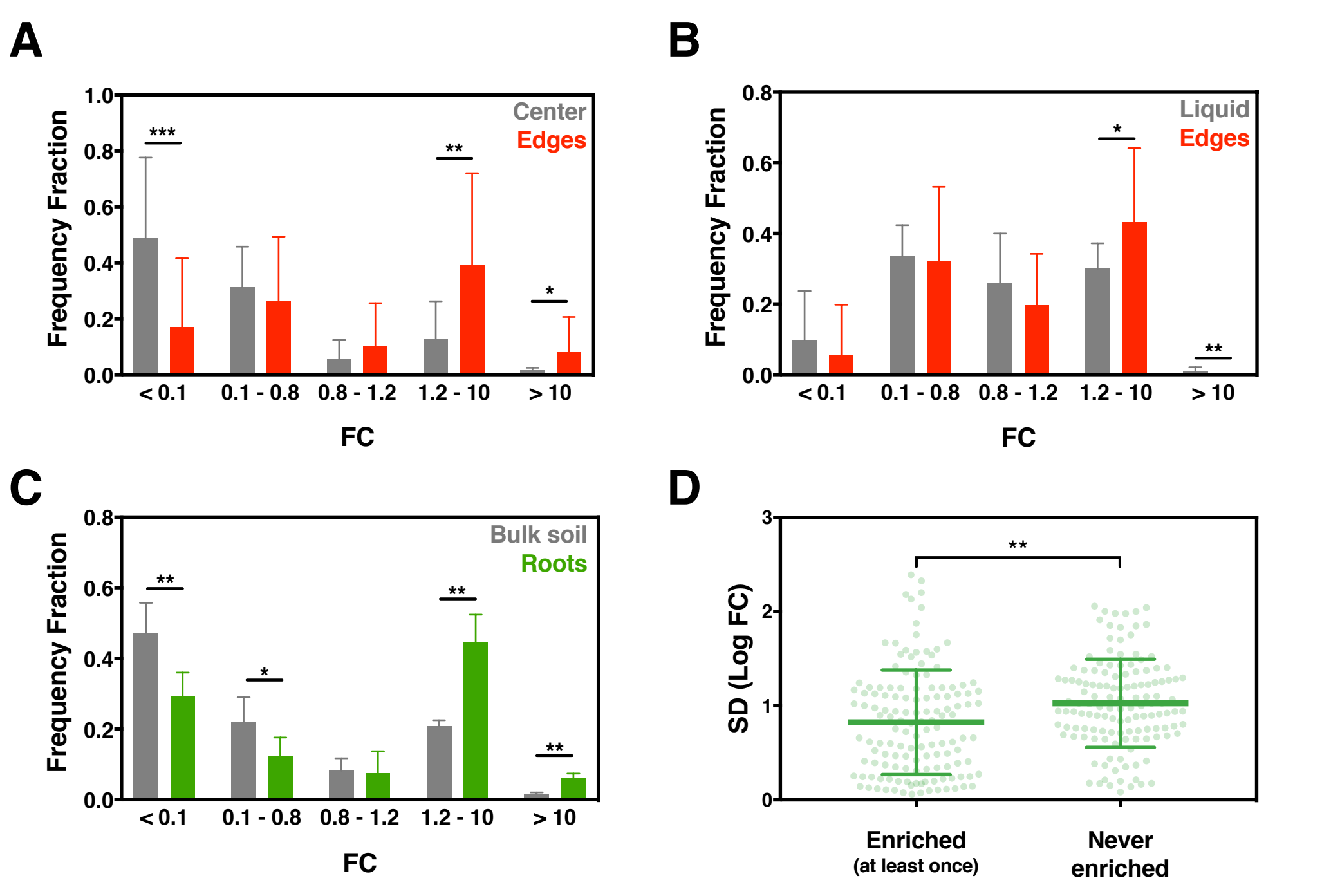
A
Frequency Fraction
1.0
0.8
0.6
0.4
0.2
0.0
Center
Edges
***
**
*
< 0.1
0.1 - 0.8
0.8 - 1.2
1.2 - 10
> 10
FC
B
Frequency Fraction
0.8
0.6
0.4
0.2
0.0
Liquid
Edges
*
**
< 0.1
0.1 - 0.8
0.8 - 1.2
1.2 - 10
> 10
FC
C
Frequency Fraction
0.8
0.6
0.4
0.2
0.0
Bulk soil
Roots
**
*
**
**
< 0.1
0.1 - 0.8
0.8 - 1.2
1.2 - 10
> 10
FC
D
SD (Log FC)
3
2
1
0
**
Enriched
(at least once)
Never
enriched

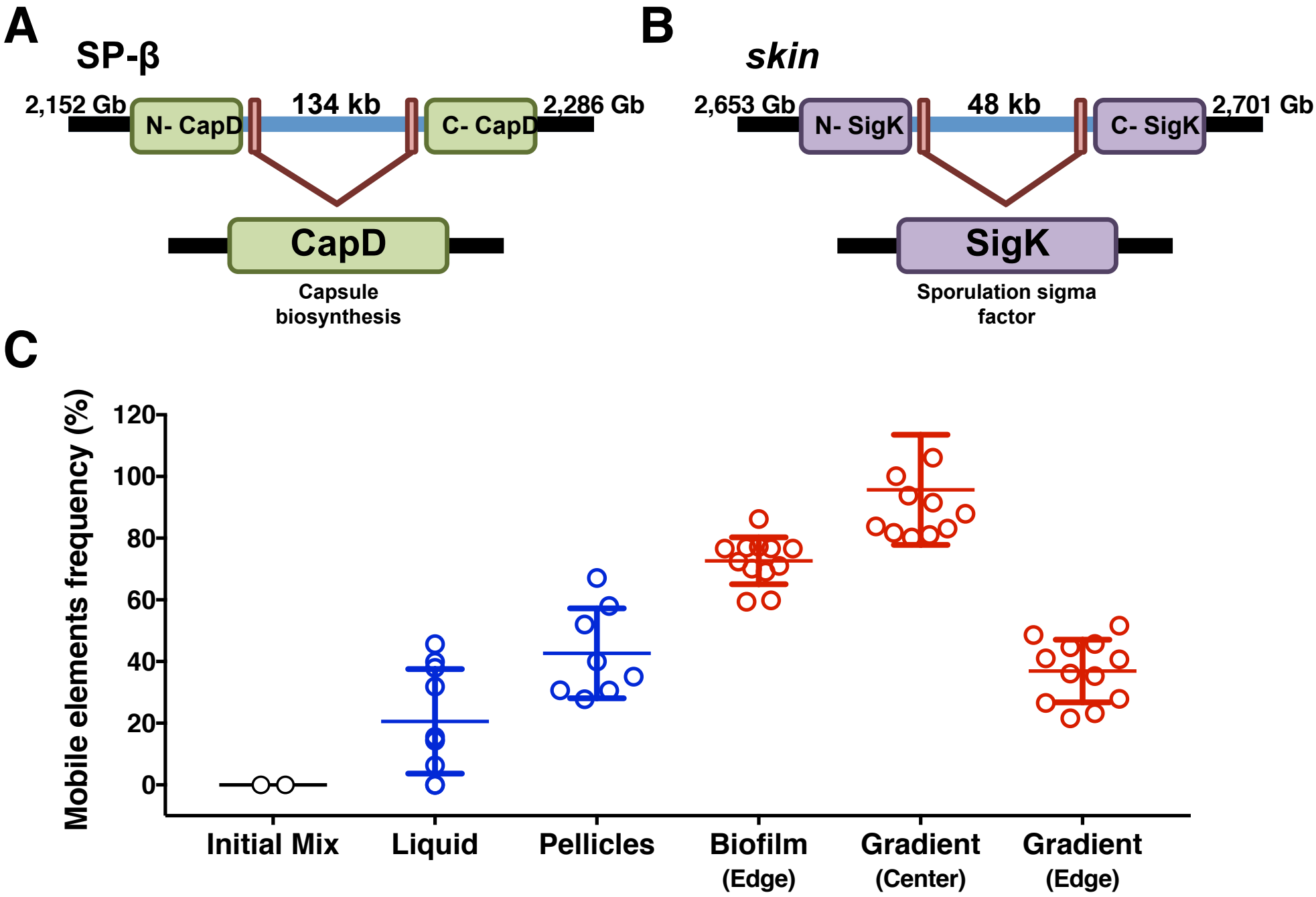
A
SP-β
2,152 Gb
N- CapD
134 kb
C- CapD
2,286 Gb
CapD
Capsule biosynthesis
B
skin
2,653 Gb
N- SigK
48 kb
C- SigK
2,701 Gb
SigK
Sporulation sigma factor
C
Mobile elements frequency (%)
120
100
80
60
40
20
0
Initial Mix
Liquid
Pellicles
Biofilm (Edge)
Gradient (Center)
Gradient (Edge)